VOL. 19, NO. 12, JUNE 2024 ISSN 1819-6608
ARPN Journal of Engineering and Applied Sciences

www.arpnjournals.com

FENI AS RAW MATERIAL FOR STAINLESS STEEL 316 AND ITS MECHANICAL PROPERTIES

Sri Endah Susilowati[1], Didit Sumardiyanto[1] and Ahmad Fudholi[2,3]
[1]Department of Mechanical Engineering, Universitas Agustus Jakarta, Jakarta, Indonesia
[2]Solar Energy Research Institute, Universiti Kebangsaan Malaysia, Bangi, Selangor, Malaysia
[3]Research Center for Energy Conversion and Conservation, National Research and Innovation Agency (BRIN), Serpong, Indonesia
E-Mail: sri.endah@uta45jakarta.ac.id

ABSTRACT

The manufacture of cast stainless steel 316 (SS 316) requires one essential raw material element, pure nickel. The demand for pure nickel is quite high, its price is the highest among other raw materials and it is still being imported. This study aims to utilise local ferronickel (FeNi) as a raw material for stainless steel and determine the effect of the percentage of FeNi usage on the mechanical properties of austenitic SS 316, which is a metal biomaterial widely used as a bone implant. This material is a potential replacement for nickel for stainless steel production. In this study, local FeNi at percentages of 0%, 23%, 45%, or 70% was added to other casting raw materials. The foundry process was carried out, and the samples were subjected to composition, tensile, hardness, and toughness tests. Results showed that all the samples had a chemical composition that met the SS 316 standard, indicating that the FeNi raw material can be used as raw material for SS 316, although impurities were still found at each percentage addition of FeNi. The tensile strength and hardness were still belowthe SS 316 standard but ductility was higher than the SS 316 standard at all percentages of FeNi.

Keywords: FeNi, SS 316, mechanical properties.

Manuscript Received 3 May 2024; Revised 14 July 2024; Published 5 September 2024

1. INTRODUCTION

Stainless steel is a steel alloy containing at least 10% chromium, which confers corrosion resistance. The annual consumption of stainless steel has increased at a compound growth rate of 5% over the last 20 years, surpassing the growth rate of other materials. Stainless steel is the most widely known metallic material, and the demand for stainless steel has increased dramatically in recent years [1–2]. Stainless steel alloys have significant uses in many industrial applications, such as aerospace, pipeline, automotive, and die and tool industries, in the form of austenitic, martensitic, ferritic, or austenoferritic (duplex); they are also used in medical devices, such as cardiovascular stents or valves, orthopedic prostheses and devices and implants used in biomedicine because of the material's malleability, resistance to corrosion and fatigue, adequate mechanical properties and excellent biocompatibility [3-7]. Thus, stainless steel has a high market potential worldwide. In Indonesia, despite the abundant nickel resources for stainless steel production, the country is still importing stainless steel from other countries.

Stainless steel categories are based on microstructures determined by chemical composition and manufacturing process [8-9]. The addition of elements, such as chromium, nickel, carbon, molybdenum, copper, nitrogen, aluminum, sulphur, and selenium, can modify the corrosion resistance, strength, ductility, machinability, and phase stability of stainless steel alloys [10-11]. Different classes of stainless steel, such as precipitation-hardening stainless steel, tool steel austenitic stainless steel [12], and maraging steels [13], are frequently used in additive manufacturing. Stainless steel can also be utilised for high-hardness and strength purposes [14] because of its relatively high strength, low density, and outstanding corrosion performance [15].

The corrosion resistance of stainless steel is primarily attributed to the formation of a protective Cr_2O_3 passive film on the alloy surface, known as passive (16-18). The film has a duplex structure and consists of an inner region rich in chromium and an outer region rich in iron. The dominant composition of passive films changes from Fe and Cr to Ni and Fe [16]. The formation of a thin protective layer on the surface and the presence of molybdenum improve performance in resisting general and localised corrosion attacks relative to other grades of austenitic stainless steel, such as 304L and 304L [17-18]. In addition, the low carbon content of stainless steel facilitates welding by decreasing carbide precipitation at grain boundaries [19]. Stainless steel 316L (SS 316L) is one of the few options for the marine, medical, and food industries, where excellent anti-corrosion properties are needed [19]. In particular, the formation of a continuous Cr_2O_3 layer in a 3 nm-thick native film after the addition of excessive amounts of Cr (>10.8 wt%) ensures long-term protection [10,11,20], enabling the alloy to withstand harsh conditions. However, the fundamental mechanism of this protection remains unclear. In other words, the critical factor in localised corrosion (such as pitting, one of the most common and severe forms of corrosion), that is, film breakdown or pitting growth stability, has been debated for decades. Frankel *et al*. [19] proposed that the protection conferred by a passive film plays an essential role under less aggressive conditions [19], and this role has been thought to be related to the impermeability of the film [21-23]. On the one hand, this idea is based on the efficient blocking of aggressive ions (e.g. chloride ions) by the compact Cr_2O_3 layer with few defects [21, 24]. On the

other hand, pitting only occurs after the protective film undergoes a breakdown event [13, 22, 25]. However, the outstanding protection might be due to the recovery (passivation) of the oxide film after film breakdown [26-27].

Stainless steel is an iron compound containing at least 10.5% chromium to prevent corrosion. This composition forms a protective layer (anti-corrosion protective layer), which is the result of spontaneous chromium oxidation. The ability to resist rust is obtained from the formation of a chromium oxide film, where the oxide layer inhibits iron oxidation. Stainless steel is a metal widely applied in medical midwife clinics. It is a Fe alloy with at least 10.5% Cr content, which is a widely used material in metallurgy because of its excellent corrosion resistance and outstanding mechanical properties. The AISI 300-series austenitic stainless steel alloys are particularly important because they show corrosion resistance superior to that of other stainless steel alloys. Moreover, some of them can be employed for biological and medical applications because of their sufficient biocompatibility [28].

SS 316L is the low-carbon version of type SS 316. The low carbon content of SS 316L (% C 0.03) minimises the deposition of damaging carbide as a result of welding. Thus, it is used when welding and maximum corrosion resistance are required. Metallic biomaterials widely used as bone implants include SS 316L. The advantages of this metal are corrosion resistance, strong mechanical properties, toughness, ductility, and cleanable surface. However, SS 316 and metal implants have drawbacks. SS 316 cannot be integrated into bones. Therefore, the surface of SS 316L must be modified by coating it with osteoconductive materials, such as hydroxyapatite (HA), which is a calcium phosphate-containing hydroxide and belongs to a mineral group. Polyvinyl alcohol, which is biocompatible and biodegradable, is used to glue HA on the surface of SS 316L [29]. Stainless steel implants used in operating rooms undergo a comprehensive product development process that closely assesses the various physical and chemical properties of the implants. Apart from ensuring the inherent stability of implants, developers must establish their compatibility with the anatomical environment [30].

This study was carried out by fabricating SS 316 from ferronickel (FeNi) raw material, which is a local product from the Ferronica Factory in Sulawesi. The results will be compared with the standard SS 316 material in terms of composition and mechanical properties. Thus, the local foundry industry can compare the advantages and disadvantages of utilizing FeNi as a raw material based on natural resources in the context of local industry independence. Smelting uses an induction furnace through the addition of other elements. Based on the standard handbook material, the composition and percentage of SS 316 are shown in Table-1 [30]. From the elemental composition in austenitic SS 316, data on the mechanical and physical properties of austenitic SS 316 are shown in Tables 2 and 3 [30].

Table-1. Chemical composition of austenitic SS 316.

Grade		C	Si	Mn	P	S	Ni	Cr	Mo	N	Fe
SS316	Min	-	-	-	-	-	10.0	16.0	2.0	-	balance
	Max	0.08	0.75	2.00	0.045	0.030	14.0	18.0	3.0	0.10	

Table-2. Mechanical properties of annealed SS 316.

Grade	UltimateTensile Strength 2% offset (MPa)	Yield Tensile Strength 2% offset(MPa)	Elongation at Break (%)	Modulus of Elasticity (GPa)
SS316	550	240	60	193

Table-3. Physical properties of annealed SS 316.

Grade	Density (g/cm^3)	Modulus Elasticity (GPa)	Electrical Conductivity ($\times 10^{-6}\Omega m$)	Thermal Conductivity (W/m.K)	Thermal Expansion ($\times 10^{-6}/K$)
SS316	8.00	193.0	0.74	16.3	15.9

2. MATERIALS AND METHODS

The raw material used was a FeNi alloy from a Sulawesi factory owned by PT. Aneka Tambang. The FeNi product is shown in Figure-1, and the composition is shown in Table-4. Given that SS 316 would be prepared, steel scrap was still needed to reduce Ni content. FeCr alloy was added to increase the Cr content. Then, other alloys, such as Mo, were added. Smelting is carried out at the stainless steel foundry factory of PT. Trieka Aimex-Cibinong.

Figure-1. FeNi from Southeast Sulawesi.

Table-4. Chemical composition of FeNi alloy.

C	Ni	Mo	Mn	Cr	Si	P	S	Cu	Fe
0.01	20.24	0.0	0.03	0.72	0.11	0.0	0.008	0.011	balance

The casting method was used, and the material balance of the input material to be entered was calculated. The results were used in obtaining the ideal stainless steel composition. The first step was to determine the weight of stainless steel, and the amount of input material was calculated and controlled until the final composition approached the composition of the SS 316 standard. When the content of an element was insufficient, other alloying elements were added. To determine the effects of changes in the addition of FeNi alloys on the mechanical properties of the product, three varieties of the material with weight percentages of 23%, 45%, and 70% of the total weight were prepared (Table 5-7).

Table-5. Chemical composition of 70% FeNi alloy.

Weight (kg)	Target	≤ 0.08	≤ 2	≤ 2	≤ 0.04	≤ 0.04	10-14	16-18	2-3
	Material	C	Si	Mn	P	S	Ni	Cr	Mo
70	FeNi	0.01	0.077	0.021	0.0	0.0	14.168	0.502	0.0
0	ScrapSteel	0.0	0.0	0.0	0.0	0.0	0.0	0.0	0.0
4	Fe - Mo	0.0004	0.0	0.0	0.0	0.0	0.0	0.0	2.46
24	Fe - Cr	0.0202	0.1296	0.0	0,005	0.0	0.0	16.2526	
0	Fe - Mn	0.0	0.0	0.0					
0	Fe - Si	0.0	0.0						
1	Ca - Si	0.0042	0.607		0.035				
100	Total	0.0527	0.946	0.9172	0.0227	0.0	10.8070	16.6596	2.62

Table-6. Chemical composition of 45% FeNi alloy.

Weight (kg)	Target	≤ 0,08	≤ 2	≤ 2	≤ 0,04	≤ 0,04	10-14	16-18	2-3
	Material	C	Si	Mn	P	S	Ni	Cr	Mo
45	FeNi	0.00	0.496	0.0135	0.0	0.0	9.106	0.567	0.0
23	Scrap SUS 304	0.0173	0.1	0.325	0.0075	0.0013	2.125	4.425	0.0
14	Scrap SUS430	0.0104	0.0016	0.106	0.0	0.0	0.045	2.499	0.0
4	Fe-Mo	0.0	0.0	0.0	0.0	0.0	0.0	0.0	2.45
14	Fe - Cr	0.0116	0.0756	0.0	0.0	0.0	0.0	9.4808	0.0
1	Ca - Si	0.0042	0.607	0.0	0.0	0.0	0.0	0.0	0.0
100	Total	0.053	0.868	0.4488	0.0075	0.0015	11.272	16.7483	2.45

Table-7. Chemical composition of 23% FeNi alloy.

Weight (kg)	Target Material	≤ 0,08 C	≤ 2 Si	≤ 2 Mn	≤ 0,04 P	≤ 0,04 S	10-14 Ni	16-18 Cr	2-3 Mo
23	FeNi	0.0	0.0264	0.0072	0.0	0.0	4.5576	0.2064	0.0
70. 68	Scrap SUS304	0.0468	0.28	0.91	0.021	0.003	6.96	12.39	0.161
4	Fe-Mo	0.004	0.0		0.02	0.005			2.46
6. 5	Fe - Cr (Ic)	0.005	0.0324	0.0	0.0016	0.0	0.0	4.0532	0.0
1	Ca - Si	0.004	0.507	0.0	0.0	0.0	0.0	0.0	0.0
105	Total	0.0527	0.946	0.9172	0.0227	0.0	10.8076	16.659	2.52

Smelting using an induction furnace by inserting scrap first after the scrap melts is added. Then, FeNi and other alloyed metals were added. Flux is added to prevent the entry of gases from the atmosphere and attract slag or impurities. The composition test was carried out by taking samples from the induction furnace before being tapped. The test was carried out with a metal analysis spectrometer. A tensile test was carried out using a universal testing machine (Servopulser Skhimadzu) with a capacity of 30 tons. A toughness test was carried out with an impact testing machine (Charpy method) with a capacity of 30 joules. Observations were made using an optical microscope and a scanning electron microscope to characterize the microstructures and phases formed in SS 316 with local FeNi raw materials and compare the microstructures and composition.

3. RESULT AND DISCUSSIONS

3.1 Chemical Composition Test Results

The results of the test of composition after melting and alloying are shown in Table-8. The composition of the product after melting met the standard limits of SS 316. High carbon content promotes the formation of nickel carbide at grain boundaries. C and Mo are important alloying elements from a corrosion point of view. The formation of carbides and their precipitation at grain boundaries cause intergranular corrosion. Hence, the amount of this element should be kept low (~0.03 wt%) [31, 32]. The presence of Mo in the alloy composition is essential for the formation of a passive film and improves pitting resistance [33]. Mo forms some oxyanions, such as molybdate, in the passive film, and these anions act as corrosion inhibitors [34]. Moreover, an intermetallic layer of MoNi forms beneath the top passive layer, increasing the level of protection and blocking the inward diffusion of aggressive ions, such as Cl [35].

Table-8. Composition test results after melting.

	C	Si	Mn	P	S	Ni	Cr	Al	Co	Cu	Nb	Mo
Standard SS316	≤ 0,08	≤ 2	≤ 2	≤ 0.04	≤ 0.04	10-14	16-18	0.0023	0.2784	0.0438	0.0418	2-3
23% FeNi	0.065	0.34	0.755	0.007	0,003	11.79	16.67	0.0033	0.2477	0.1016	0.0394	2.261
45% FeNi	0.08	0.776	0.296	0.005	0,003	12.77	16.91	0.0031	0.2364	0.1596	0.0396	2.087
70% FeNi	0.08	0.499	0.517	0.004	0,006	14.45	16.90	0.0035	0.1863	0.1696	0.0395	2.090

Brittleness in the grain boundaries is prevented by maintaining low content of phosphorus and sulphur. High phosphorus content is detrimental mainly because of the segregation of phosphorus to grain boundaries after phosphorus is fully rejected from the retained austenite; this process may lead to embrittlement and decreases corrosion resistance [29, 30, and 36]. The Ni content in the product for the three composition varieties reaches the standard value. As an alloying element, nickel enhances important properties, such as formability, weldability, and ductility, while increasing corrosion resistance in some applications [37, 38]. Nickel enhances weld filler, and the optimum heat input increases the amount of absorbed energy by improving ductility attributed to austenite enrichment in the duplex stainless steel weld [39, 40].

Cr, Mo, and N are important alloying elements for passive film formation and repassivation, but their roles in the passive film have not been fully explored. Resistance to localised corrosion may be attributed to the repassivation of the passive film and its stability [40]. (E). The Cr content for the three composition varieties reaches the standard value. Cr (10.5%) must be present in passive layer formation. Austenitic SS 316 contains 16%-18% Cr and has a thick passive layer that confers high resistance to corrosion. In general, Cr content is the primary factor determining the corrosion resistance of stainless steel [26-29].

Molybdenum plays an active role in corrosive resistance, especially pitting and crevice corrosion, and enhanced performance in pitting resistance and repassivation potential [41-43]. Alloying Mo enhances the pitting corrosion resistance of alloys by increasing the level of protection conferred by the passive film and lowering the pit growth rate. Molybdate ions can inhibit pitting corrosion in chloride-containing solutions by elevating the pitting and showing enhanced performance in pitting resistance and repassivation potential [30-33, 41, 44-45]. Mo can enhance pitting resistance, and pitting can be eliminated with the addition of Mo between 4 at. % to 8 at. %, coherent interfaces and their composition transition explain the excellent wear and corrosion improvement of the coatings [43]. SS 316L has good corrosion resistance and mechanical qualities owing to the inclusion of elements, including Mo, Ni, and Cr [46]. Table-8 shows the amount of Mo content in the three variations of the product composition that reach the standard value for SS 316 composition.

Mn is required, but the maximum content is limited to 2% (Table-8). It has almost the same function as Ni. One of the benefits of Mn is that it confers abrasion resistance on stainless steel. However, Mn easily interacts with the environment containing S and forms manganese sulphide compounds [29].

3.2 Tensile Test Results

Table-9 shows the results of tensile tests on stainless steel with local FeNi raw materials for each percentage of FeNi. As shown in Table-9, the tensile strength tends to increase with increasing local FeNi content although it remains below the standard SS 316 tensile strength and 0% FeNi. Likewise, the yield strength appears to have a tendency that is almost the same as the tensile strength, where the yield strength of products made from local FeNi tends to increase with FeNi content. Thus, the addition of FeNi increases the tensile strength and yield strength of the product. The extension is only 45% FeNi, which is above the standardSS 316 steel.

Table-9. Tensile test results on each percentage of local FeNi.

% Ni	σuts (kg/mm^2)	σyield (kg/mm^2)	e (%)
SS 316	59.0	29.5	50.0
0 % Fe-Ni	53.8	28.4	40.9
23 % Fe-Ni	49.0	21.0	47.1
45 % Fe - Ni	49.0	21.0	54.3
70 % Fe - Ni	52.0	23.0	44.2

Table-9 shows the highest tensile strength of 70% local FeNi, namely, 52 kg/mm^2 (below the minimum standard of 59 kg/mm2), whereas the elongation is lower than that of 23% FeNi and 45% FeNi. The possible reason is that the 70% FeNi content of C is quite larger than 23% FeNi. Tensile strength and elongation are largely dependent on porosity rather than on grain size because the fracture is mainly induced by microvoid growth as porosity decreases and tensile strength and elongation increase [46]. Porosity occurs because of gas diffusion and turbulent flow when the material is poured into the mold because of gating system errors. Porosity results in stress concentration at the edges, and thus the material will fail before reaching its theoretical stress. Porosity reduces ductility. This effect can be observed at the local FeNi composition of 23% and 45%. In general, the yield strength, tensile strength, and elongation of sintered materials should increase with decreasing porosity [47]. The reduced porosity in the as-sintered conditions results in 15% and 5% improvement in tensile yield and ultimate tensile strengths, respectively [48].

3.3 Hardness Test Results

The test results of stainless cast steel made for each local FeNi percentage (Table 10 and Figure-2). Table 10 and Figure-2 show that the hardness of the composition fails to meet the standard SS 316 hardness standard, namely, 170 BHN. This value tends to decrease with increasing local FeNi percentage. The hardness values for 23% FeNi, 45% FeNi, and 70% FeNi are 144.00, 135.00 and 142 BHN, respectively. The material with 45% FeNi has the lowest hardness (135 BHN) despite having a high carbon content (0.08% C) because of numerous ferrite phases, and the number of inclusions affects the hardness of metals.

Table-10. Hardness test results for stainless steel.

% FeNi	Tracking	d (average)	BHN	BHN (average)
SS316 standard			170.00	170.00
0% FeNi		1.2563	140.65	140.65
23% FeNi	1		144.00	144.00
	2	1.2615	143.00	
	3	1.2560	144.00	
	4	1.2559	144.00	
	5	1.2517	145.00	
45 % Fe Ni	1	1.2970	135.00	135.00
	2	1.3005	134.00	
	3	1.2973	135.00	
	4	1.3000	134.00	
	5	1.2971	135.00	
70 % FeNi	1	1.2655	142.00	142.00
	2	1.2600	143.00	
	3	1.2564	144.00	
	4	1.2645	142.00	
	5	1.2650	142.00	

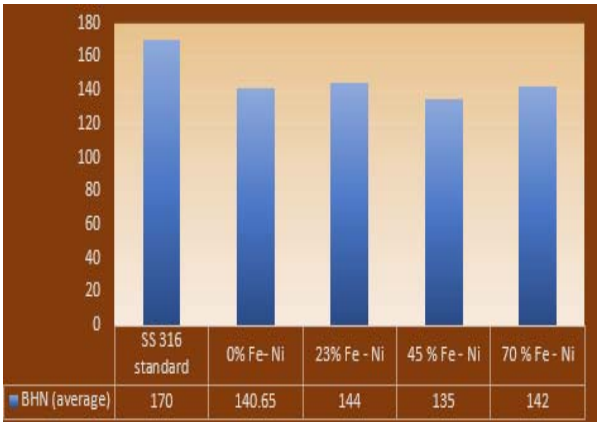

Figure-2. Hardness test results.

3.4 Impact Test Results

Impact testing carried out by the Charpy method produces impact energy prices and impactprices as shown in Table-11. The results of the impact test show that the highest impact value occurs in steel with a composition of 45% FeNi, which is 280 Joules or 3,110 Joules/mm^2. This means that the cast steel is more ductile than the others. All samples have a higher impact value than standard SS 316 steel (94.7 Joules), this means that the resulting material is also more ductile than standard SS 316 steel. In general, it can be said that the lower the FeNi content, the higher the impact price. In the composition of 23% FeNi, the lowest impact value is 140 Joules. This is presumably due to the large number of inclusions contained in 23% FeNi. Inclusions generally have hard and brittle properties.

Table-11. Impact test results.

Sample	A (mm^2)	Impact Energy (Joule)	Impact Strength (Joule/mm^2)
SS316 Standard	-	94.7	-
0 % Fe-Ni		287.2	
23 % Fe-Ni	85	140.0	1.647
45 % Fe-Ni	90	280.0	3.110
70 % fe-Ni	87	268.0	3.080

3.5 Microstructure Observation

The results of structural observations for each percentage of FeNi are shown in Figures 3 and 4. The sample contains impurities (indicated by small black dots), affect the properties of the resulting material. In the microstructure photographs, impurities or impurity elements on the austenite matrix are indicated by the presence of black spots. Stainless steel made with 70% FeNi has few impurities, which are scattered in the matrix. In the 23% and 45% FeNi samples, the impurities increase. In the 0% FeNi sample, impurities are slightly visible and scattered. The amount of impurities increases with decreasing level or percentage of FeNi. Such an increase affects the properties of materials [49].

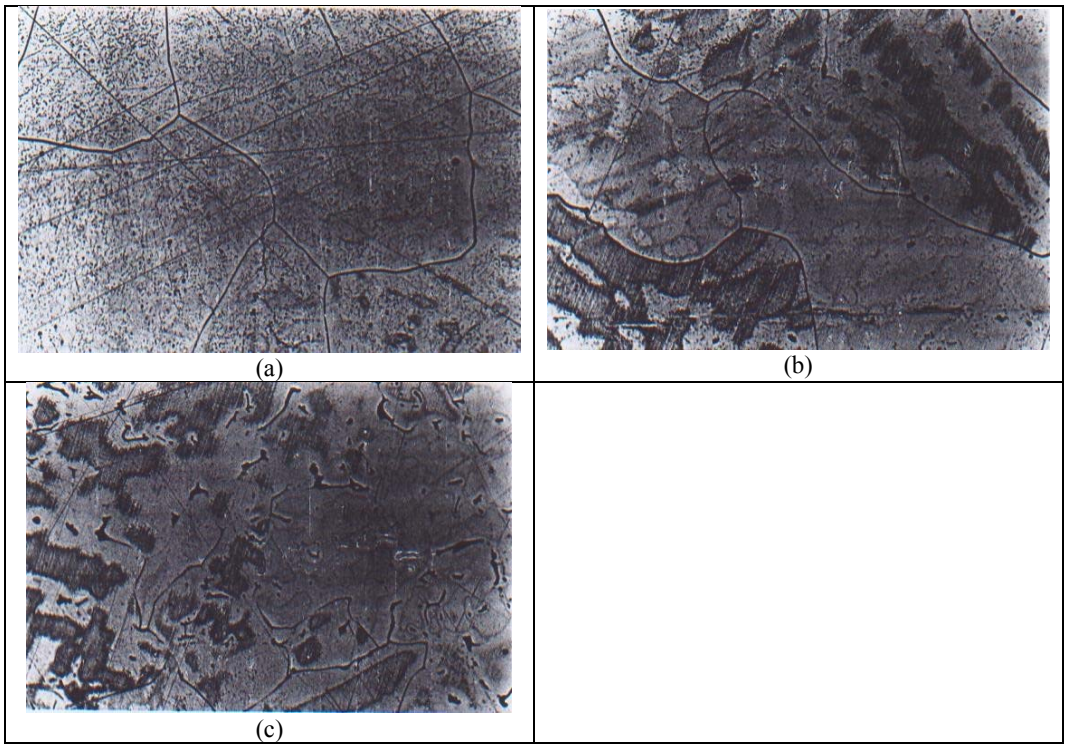

Figure-3a. The results of structural observations for each percentage of FeNi; (a) microstructure 23% local FeNi alloy (100×), (b) microstructure 45% local FeNi alloy (100×), and (c) microstructure 70 % local FeNi Alloy (100×).

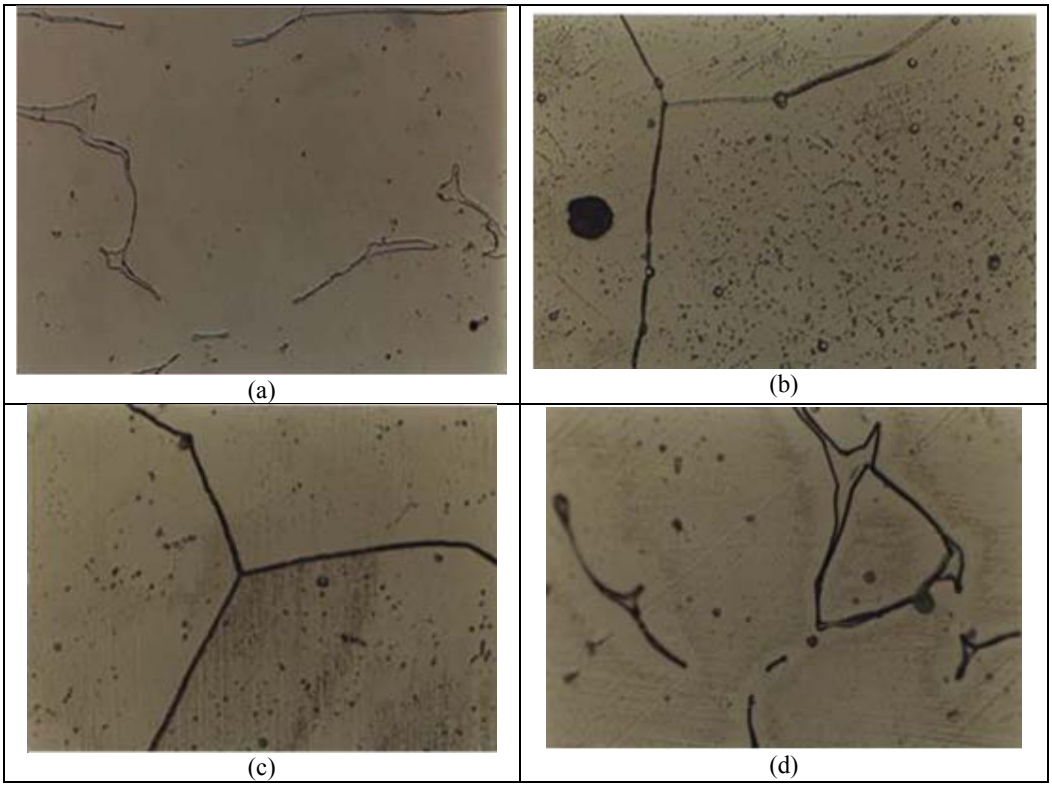

Figure-4. Optical Microscope image magnification 500×: (a). 0% local FeNi alloy (b). 23% local FeNi alloy (c). 45% local FeNi alloy (d). 70% local FeNi alloy

4. CONCLUSIONS

The results showed that all the samples had a chemical composition meeting the SS 316 standard, indicating that the FeNi raw material can be used as raw material for SS 316 stainless steel, although impurities were still found in each percentage addition of FeNi. At all percentages of FeNi, the tensile strength and hardness obtained were still below the SS 316 standard, but the ductility exceeded the SS 316 standard. The microstructure showed black spots and thick grain boundaries. These black spots were CaO and MgO, whereas the thick grain boundaries were chromium carbide and nickel carbide.

REFERENCES

[1] Cobb Harold M. 2008. Stainless Steels: A Steel Products Manual. Association for Iron & Steel Technology.

[2] Marcus, Philippe (ed.). 2011. Corrosion mechanisms in theory and practice. CRC press.

[3] Baddoo N. R. 2008. Stainless steel in construction: A review of research, applications, challenges and opportunities. Journal of constructional steel research. 64.11: 1199-1206.

[4] M. K. Alam, M. Mehdi, R. J. Urbanic, A. Edrisy. 2020. Mechanical behavior of additive manufactured AISI 420 martensitic stainless steel, Mater. Sci. Eng. A 773: 138815.

[5] Esmaeili A., Ghaffari S. A., Nikkhah M., Ghaini F. M., Farzan F. & Mohammadi S. 2021. Biocompatibility assessments of 316L stainless steel substrates coated by Fe-based bulk metallic glass through electro-spark deposition method. Colloids and Surfaces B: Biointerfaces. 198, 111469.

[6] Bekmurzayeva Aliya, *et al*. 2018. Surface modification of stainless steel for biomedical applications: Revisiting a century-old material. Materials Science and Engineering: C. 93: 1073-1089.

[7] Wang Niyou, *et al*. 2021. Cytotoxicity of Ti/SS316/Mg Particles on Human Osteoblasts. In: Materials Science Forum. Trans Tech Publications Ltd. pp. 128-133.

[8] C.-O. Olsson, D. Landolt. 2003. Passive films on stainless steel chemistry, structure, and growth, Electrochim. Acta. 48: 1093-1104.

[9] G. Sander, S. Thomas, V. Cruz, M. Jurg, N. Birbilis, X. Gao, M. Brameld, C. Hutchinson. 2017. On the corrosion and metastable pitting characteristics of 316L stainless steel produced by selective laser melting, J. Electrochem. Soc. 164: C250-C257.

[10] A. Al-Amr. 2005. Mechanical Behavior and Structure of Passive Films on Austenitic Stainless Steels.

[11] J. R. Davis. 1994. Stainless Steels, ASM international.

[12] H. D. Carlton, A. Haboub, G. F. Gallegos, D. Y. Parkinson, A. A. MacDowell. 2016. Damage evolution and failure mechanisms in additively manufactured stainless steel, Mater. Sci. Eng. A 651: 406-414.

[13] G. Casalino, S. Campanelli, N. Contuzzi, A. Ludovico. 2015. Experimental investigation and statistical optimisation of the selective laser melting process of maraging steel, Opt. Laser Technol. 65: 151-158.

[14] T. D. Ngo, A. Kashani, G. Imbalzano, K. T. Nguyen, D. Hui. 2018. Additive manufacturing (3D printing): a review of materials, methods, applications, and challenges, Compos. Part B Eng. 143: 172-196.

[15] Ettefagh, Ali Hemmasian, Guo, Shengmin, Raush, Jonathan. 2021. Corrosion performance of additively manufactured stainless steel parts: A review. Additive Manufacturing. 37: 101689.

[16] JIN Zuquan, *et al*. 2022. Passivation and depassivation properties of Cr-Mo alloyed corrosion-resistant steel in simulated concrete pore solution. Cement and Concrete Composites. 126: 104375

[17] Peguet L., Gaugain A., Dussart C., Malki B., Baroux B. 2012. Statistical study of the critical pitting temperature of 22-05 duplex stainless steel. Corros. Sci. 60, 280-283. [CrossRef]

[18] Punckt C., Bolscher M., Rotermund H., Mikhailov A., Organ L., Budiansky N., Scully J., Hudson J. 2004. The sudden onset of pitting corrosion on stainless steel is a critical phenomenon. Science. 305, 1133-1136. [CrossRef]

[19] Frankel G., Li T., Scully J. 2017. Perspective-Localized Corrosion: Passive Film Breakdown vs. Pit Growth Stability. J. Electrochem. Soc. 164, C180-C181. [CrossRef]

[20] Kim E., Ishtiaq M., Han J.C., Ko K., Bae H., Sung H., Kim J., Seol J. 2021. Near atomic-scale comparison of passive film on a 17 wt% Cr-added 18 wt% Mn steel

with those on typical austenitic stainless steels. Scripta Mater. 203, 114112. [CrossRef]

[21] Sun J., Tang H., Wang C., Han Z., Li S. 2022. Effects of Alloying Elements and Microstructure on Stainless Steel Corrosion: A Review. Steel Res. Int. 93, 2100450. [CrossRef]

[22] Natishan P., O'Grady W. 2014. Chloride Ion Interactions with Oxide-Covered Aluminum Leading to Pitting Corrosion: A Review. J. Electrochem. Soc. 161, C421–C432. [CrossRef]

[23] Marcus P., Maurice V., Strehblow H. 2008. Localized corrosion (pitting): A model of passivity breakdown including the role of the oxide layer nanostructure. Corros. Sci. 50, 2698-2704. [CrossRef]

[24] Brooks A., Clayton C., Doss K., Lu Y. 1986. On the Role of Cr in the Passivity of Stainless Steel. J. Electrochem. Soc. 133, 2459-2464. [CrossRef]

[25] Maurice V., Yang W., Marcus P. 1998. X-ray photoelectron Spectroscopy and Scanning Tunneling Microscopy Study of Passive Films Formed on (100) Fe-18Cr-13Ni Single-Crystal Surfaces. J. Electrochem. Soc. 145, 909-920. [CrossRef]

[26] Anderko A., Sridhar N., Yang L., Grise S., Saldanha B., Dorsey M. 2005. Validation of localised corrosion model using real-time corrosion monitoring in a chemical plant. Corros. Eng. Sci. Technol. 40, 33-42. [CrossRef]

[27] Xie Y., Artymowicz D., Lopes P., Aiello A., Wang D., Hart J., Anber E., Taheri M., Zhuang H., Newman R., *et al*. 2021. A percolation theory for designing corrosion-resistant alloys. Nat. Mater. 20, 789-793. [CrossRef]

[28] Bertero E., Hasegawa M., Staubli S., Pellicer E., Herrmann I. K., Sort J. ... & Philippe L. 2018. Electrodeposition of amorphous Fe-Cr-Ni stainless steel alloy with high corrosion resistance, low cytotoxicity, and soft magnetic properties. Surface and Coatings Technology. 349, 745-751.

[29] Tenong, F. F. S. B., Hikmawati, D., & Setiawati, E. M. (2021, February). Characterization of Vickers hardness and corrosion rate of stainless steel-316L coated with hydroxyapatite-polyvinyl alcohol. In Journal of Physics: Conference Series (Vol. 1816, No. 1, p. 012012). IOP Publishing.

[30] Walley K. C., Bajraliu M., Gonzalez T., Nazarian A. & Goulet J. A. 2016. The chronicle of a stainless steel orthopedic implant. The Orthopaedic Journal at Harvard medical school. 17, 68-74.

[31] Moosbrugger C., Sanders B. R., Anton G. J., Hrivnak N., Kinson J., Polakowski C. & Scott Jr W. W. 2003. ASM handbook (Vol. 13). S. D. Cramer & B. S. Covino Jr (Eds.). Materials Park, Ohio: ASM international.

[32] J. Gubicza, M. El-Tahawy, Y. Huang, H. Choi, H. Choe, J.L. L´ab´ar, T.G. Langdon. 2016. Microstructure, phase composition and hardness evolution in 316L stainless steel processed by high-pressure torsion, Mater. Sci. Eng. A 657: 215-223.

[33] S. M. Yusuf, M. Nie, Y. Chen, S. Yang, N. Gao. 2018. Microstructure and corrosion performance of 316L stainless steel fabricated by selective laser melting and processed through high-pressure torsion, J. Alloy. Compd. 763: 360-375.

[34] M. A. Bevan, A. Ameri, D. East, D. Austin, A. Brown, P. Hazell, J. Escobedo-Diaz. 2017. Mechanical properties and behavior of additive manufactured stainless steel 316L. Characterization of Minerals, Metals, and Materials, Springer. pp. 577-583.

[35] J. R. Trelewicz, G. P. Halada, O. K. Donaldson, G. Manogharan. 2016. Microstructure and corrosion resistance of laser additively manufactured 316L stainless steel, Jom. 68: 850-859.

[36] G. Halada, C. Clayton. 1993. Comparison of Mo-N and W-N synergism during passivation of stainless steel through x-ray photoelectron spectroscopy and electrochemical analysis, J. Vac. Sci. Technol. A Vac. Surf. Films. 11: 2342-2347.

[37] Tian H., Cheng X., Wang Y., Dong C. & Li X. 2018. Effect of Mo on the interaction between α/γ phases of duplex stainless steel. Electrochimica Acta. 267, 255-268.

[38] Lotfi N., *et al*. 2018. Zinc–nickel alloy electrodeposition: Characterization, properties, multilayers and composites. Protection of metals and physical chemistry of surfaces. 54: 1102-1140.

[39] Breu C. M., Cristóbal M. J., Losada R., Nóvoa X. R., Pena G. & Pérez M. C. 2004. Comparative study of passive films of different stainless steels developed on

alkaline medium. Electrochimica Acta. 49(17-18): 3049-3056

[40] Ibrahim O. H., Ibrahim I. S., Khalifa T. A. F. 2010. Impact behavior of different stainless steel weldments at low temperatures. Eng Fail Anal. 17: 1069-76.

[41] Lee Jae-Bong. 2006. Effects of alloying elements, Cr, Mo, and N on repassivation characteristics of stainless steels using the abrading electrode technique. Materials Chemistry and Physics. 99.2-3: 224-234.

[42] Cwalina, K. Lutton, *et al*. 2019. Revisiting the effects of molybdenum and tungsten alloying on corrosion behavior of nickel-chromium alloys in aqueous corrosion. Current Opinion in Solid State and Materials Science. 23.3: 129-141

[43] Bocher F., Huang R., Scully J. R. 2010. Prediction of critical crevice potentials for Ni-Cr-Mo alloys in simulated crevice solutions as a function of molybdenum content. Corrosion, 2010, 66.5: 055002-055002-15.MCCAFFERTY, Edward. Introduction to corrosion science. Springer Science & Business Media.

[44] Ostovan Farhad, *et al*. 2021. On the role of molybdenum on the microstructural, mechanical, and corrosion properties of the GTAW AISI 316 stainless steel weld. Journal of Materials Research and Technology. 13: 2115-2125

[45] Jiang Di, et al. 2022. Synergistic improvement of wear and corrosion resistance of CoCrNiMoCB coatings obtained by laser cladding: Role of Mo concentration. Materials & Design. 219: 110751.

[46] Yoon Tae Shik, *et al*. 2003. Effects of sintering conditions on the mechanical properties of metal injection molded 316L stainless steel. ISIJ international. 43.1: 119-126.

[47] A. Salak. 1995. Ferrous Powder Metallurgy, Cambridge International Science Publishing, Cambridge. 102.

[48] Kumar Punit, *et al*. 2023. Tensile and fatigue properties of the binder jet printed and hot isostatically pressed 316L austenitic stainless steel. Materials Science and Engineering: A. 868: 144766

[49] Gotow Takahiro, *et al*. 2017. Effects of impurity and composition profiles on electrical characteristics of GaAsSb/InGaAs hetero-junction vertical tunnel field effect transistors. Journal of Applied Physics. 122.17: 174503.